Journal of
Synchrotron
Radiation

ISSN 0909-0495

Received 25 June 2004
Accepted 23 November 2004

A new cell for temperature-dependent X-ray absorption spectroscopy of liquid solutions: application to $PbBr_2$ solutions in diethylene glycol

D. Lützenkirchen-Hecht,[a]* T. Oldag,[b] P. Keil,[a] H.-L. Keller[b] and R. Frahm[a]

[a]Institut für Materialwissenschaften und Fachbereich C, Mathematik und Naturwissenschaften, Bergische Universität Wuppertal, Gaußstraße 20, D-42097 Wuppertal, Germany, and [b]Fachbereich Chemie, Universität Dortmund, Otto-Hahn-Straße 6, D-44227 Dortmund, Germany. E-mail: dirklh@uni-wuppertal.de

An *in situ* cell has been constructed for temperature-dependent X-ray absorption experiments (EXAFS and XANES) of lead bromine ($PbBr_2$) solutions in diethylene glycol in the temperature range from room temperature up to about 433 K. The solution is kept in a thermostated container made of carbon-reinforced teflon between two thin chemically inert quartz glass windows with a high transmission for hard X-rays. The construction of the cell ensures that these X-ray windows are thermalized so that any possible precipitation of solid products from the solution is inhibited. The cell consists mainly of two hermetically sealed teflon containers for the thermostating fluid (silicon oil) that were fitted together in such a way that a small and variable volume ($\sim$2–4 cm^3) for the liquid under investigation was achieved. A small thermocouple in a glass enclosure was placed in the solution to maintain temperature control and feedback to the thermostat. The cell design and its performance for temperature-dependent *in situ* investigations with X-rays are reported. Some preliminary results obtained for $PbBr_2$ solutions in diethylene glycol are given.

Keywords: high-temperature cell; $PbBr_2$ solutions; EXAFS; solubility.

1. Introduction

The speciation of metal ions in high-temperature high-pressure aqueous solutions is important in many geochemical, geothermal and environmental processes including metal transport and ore formation (see, for example, Farges *et al.*, 1993; Oelkers *et al.*, 1998; Charnock *et al.*, 1999; Ragnarsdottir *et al.*, 1998; Seward *et al.*, 1996). Solvated metal ions play an essential role in the treatment of liquid nuclear waste (Rothe *et al.*, 2002) and the understanding of their sorption mechanisms by humic substances (Kemner *et al.*, 1995; Denecke *et al.*, 1998). Temperature-dependent measurements are of fundamental interest for a detailed understanding of the dynamics and the interactions between the solvent and the ions, and changes in this solvation-shell environment play a significant role in many physicochemical aspects of hydrothermal solutions. Furthermore, liquids at elevated temperatures and pressures are also important for heterogeneous catalysis (*e.g.* Schneider *et al.*, 2003). In the past, X-ray diffraction (XRD), providing the contributions of all pair distribution functions of the sample, has proven to give detailed structural data of liquids also (see, for example, Palinkas & Kalman, 1981), especially if the anomalous scattering technique is applied, so that the contributions of the different atomic pair correlation functions can be separated more easily (Kortright *et al.*, 1983; Schultz *et al.*, 1990). However, such diffraction measurements are extremely time-consuming and highly concentrated samples are essential, especially for the application of anomalous scattering techniques (see, for example, Kortright *et al.*, 1983; Schultz *et al.*, 1990).

For more dilute sample systems, diffraction experiments can hardly provide sufficient information about the structure of solved metal ions. In this context, the X-ray absorption fine-structure spectroscopy technique (XAFS) is an element-specific method of obtaining structural information. XAFS explores the modulations of the X-ray absorption coefficient above the absorption edge of a given element. It is caused by the scattering of the ejected photoelectron waves from neighbouring atoms, *i.e.* XAFS cannot provide long-range-order structural information. However, EXAFS has furthered our basic understanding of amorphous substances, glasses and liquids owing to its ability to specify the accurate local short-range structure around the X-ray absorbing atom (see, for example, Koningsberger & Prins, 1988; Kemner *et al.*, 1995; Seward *et al.*, 1996; Tsutsui *et al.*, 1997; Licheri & Pinna, 1983; Lützenkirchen-Hecht *et al.*, 1998; Oelkers *et al.*, 1998; Charnock *et al.*, 1999; Lützenkirchen-Hecht & Frahm, 2001). A review dealing with the application of EXAFS to liquid

systems with the focus on high-temperature and high-pressure studies was recently given by Filipponi (2001).

In summary, the ability of EXAFS to elucidate precisely the structural environment of a selected anion or cation is especially useful if the atom has a specific bond geometry such as in many humic or other organic solutions (see, for example, Riggs-Gelasco *et al.*, 1995; Gharia *et al.*, 1995; Della Longa *et al.*, 1995; Yachandra *et al.*, 1996). Despite their importance, however, the majority of X-ray absorption studies are focused on aqueous solutions and few investigations have dealt with organic solvents. From a fundamental point of view, the solvation of metals in organic solutions is of special interest. In the case of $PbBr_2$ in diethylene glycol, an exceptional behaviour of the solubility as a function of the temperature was observed as follows. Usually the solubility of a salt in a solvent increases continuously as a function of the temperature, as can be seen in Fig. 1 for $PbBr_2$ in water or ethylenelycol (Hertz & Hellebrandt, 1923; Oldag, 2000). However, for $PbBr_2$ in diethylene glycol, a distinct solubility maximum with about 130 mg ml^{-1} at about 357 K was observed, compared with 25 mg ml^{-1} and 75 mg ml^{-1} at 303 and 443 K, respectively (see Fig. 1). Solid structures which were precipitated from solutions that were previously held at temperatures below and above the observed solubility maximum reveal completely different crystallographic structures with changing chemical compositions: for $T < 357$ K, *in situ* X-ray diffraction experiments have proven that the precipitate consists of $PbBr_2 \cdot C_4H_{10}O_3$. This chemical compound is spontaneously formed after addition of $PbBr_2$ to pure diethylene glycol and stable also after cooling to room temperature. For more elevated temperatures above 357 K, a sediment of pure $PbBr_2$ is always present according to temperature-dependent X-ray diffraction experiments. However, if such a preheated solution is cooled down to room temperature, a structure consisting of 7 $PbBr_2 \cdot 8\ C_4H_{10}O_3$ is formed, *i.e.* although the sediment is free of any solvent for temperatures above 357 K, the precipitate is enriched in the diethylene glycol solvent compared with the low-temperature

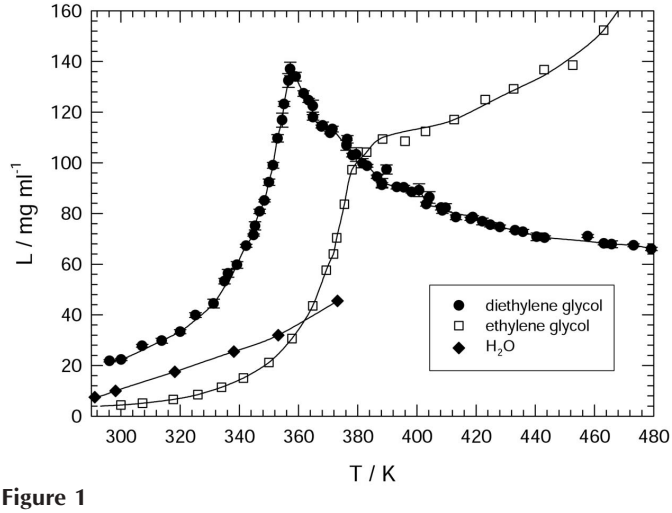

Figure 1
Solubility of $PbBr_2$ determined by refined potentiometric titration using EDTA (Oldag *et al.*, 2005) in different solvents as indicated (Oldag, 2000).

precipitates (Oldag *et al.*, 2005). The kinetics of the crystallization for each of the two structures varies significantly from several hours to several weeks. Together with the temperature dependence of the solubility, this is a clear indication for structural changes of the lead bromine complexes in the solution.

We therefore have conducted an *in situ* X-ray absorption study of the temperature-dependent behaviour of $PbBr_2$ diethylene glycol solutions. In order to obtain reliable results, a careful adjustment and control of the solution temperature is required and, at the same time, side reactions of the reactive solution with cell materials as well as a possible precipitation of soluble species at the necessary X-ray windows must be avoided. On the other hand, the sample has to be confined in a geometry suitable for the X-ray measurements, *i.e.* with a sufficient transmission and absorption change at the edges under investigation. In the past, cells coming from other spectroscopies such as UV-Vis, Raman or IR-absorption have been used or adapted for X-ray absorption experiments (*e.g.* Villain *et al.*, 1993); nevertheless, these cells are not suited for the solvents processed in this study for several reasons discussed below in more detail. Details of relatively simple cells for XAFS investigations have been published (*e.g.* Sanchez Marcos *et al.*, 1994); however, those cannot be adapted to experiments at higher temperatures owing to the use of, for example, organic polymer films such as polypropylene, Mylar (polyethylene terephthalate) or Kapton (polyimide) as X-ray windows (Furenlid *et al.*, 1990; Sanchez Marcos *et al.*, 1994). While these window materials are suited for aggressive or corrosive aqueous solutions (*e.g.* Lützenkirchen-Hecht *et al.*, 1998), they are not suited for the organic solvents and the elevated temperatures used in the present study owing to their chemical instability against the diethylene glycol solvent. Furthermore, these cells cannot avoid possible interactions of the solvent with air or humidity from the laboratory atmosphere. Other cells make use of mechanically stable and heat-resistant but relatively thick X-ray windows of more than 1 mm thickness (Seward *et al.*, 1996; Charnock *et al.*, 1999) that are not applicable in the X-ray range below $\sim$15 keV owing to their increased parasitic absorption and small gap of some 100 µm of liquid between the two windows. Another technique that has been widely applied for the investigation of liquids under increased pressure and temperature is the dispersion of small particles of a condensed liquid in a matrix (*e.g.* inert powders, wax, glue *etc.*). Above the melting point of the sample under investigation, the sample particles transform into a collective of micrometric droplets embedded in the matrix (see, for example, Ottaviano *et al.*, 1994, or Filipponi & Di Cicco, 1994). However, such an approach is not possible in the present case, since the formation of a thermal equilibrium between a soluted material and the solvent cannot be achieved in the case of more or less isolated droplets, and remaining fractions of solid material may affect or even perturb the X-ray measurements. Filipponi and co-workers have shown that thin quartz glass windows of about 100 µm thickness are suited for the confinement of liquid Br_2 (Filipponi *et al.*, 1993). In this contribution we

report the design and the construction of a new high-temperature cell with thin quartz windows for X-ray investigations of liquids in the temperature range from room temperature to about 433 K. First results on $PbBr_2$ diethylene glycol solutions with XAFS at the Br *K*-edge and the *L*-edges of Pb will be presented.

2. Cell design

For the *in situ* and temperature-dependent XAFS experiments a novel *in situ* cell was constructed (see Fig. 2). An indispensable requirement for the planned experiments was the use of chemically inert materials to ensure that there are no side reactions of the heated solutions with the cell itself that may alter the structure of the solution and lead to erroneous results. Therefore the body of the new cell was completely made of carbon-reinforced Teflon (PTFE). Two thin quartz glass plates (each ~180 µm thickness) with an X-ray transmission between ~52% at the Pb L_3-edge at 13035 eV and 71% at the L_1-edge (15861 eV) served as X-ray windows. Even experiments at lower X-ray energies are feasible with the used window materials; for example, the transmission of the windows is about 30% at 10 keV, while cells employing fused silica windows of more than 1 mm thickness are restricted to X-ray energies above ~25 keV (Seward *et al.*, 1996; Oelkers *et al.*, 1998; Charnock *et al.*, 1999).

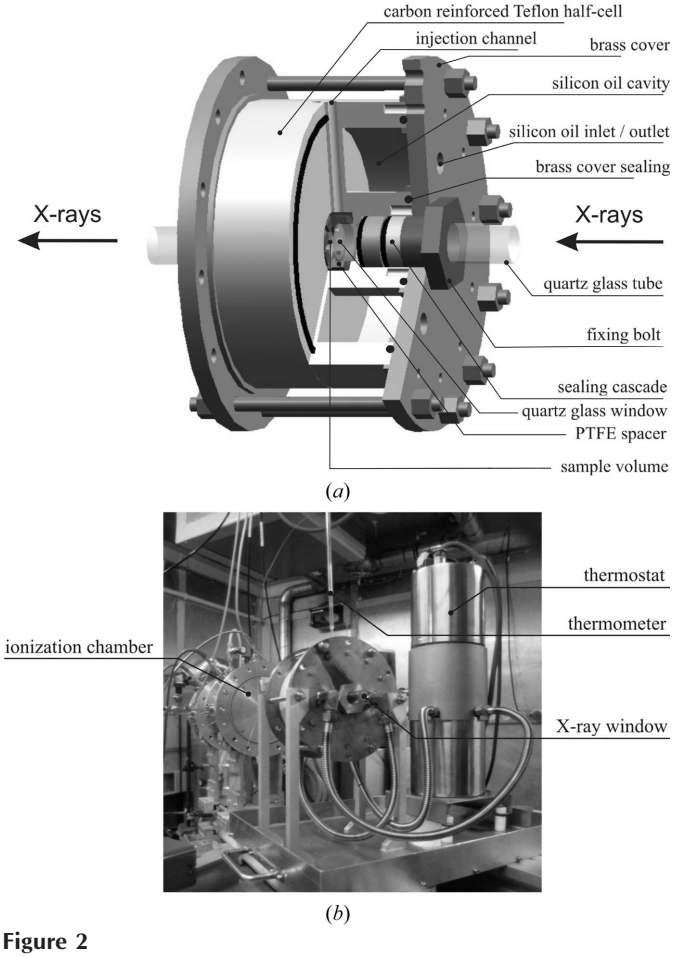

Figure 2
(*a*) Schematical view of the high-temperature *in situ* cell for X-ray investigations of liquids (partly as a sectional drawing) and (*b*) experimental set-up at the RÖMO II beamline at HASYLAB. Some essential parts are marked by arrows. Refer to the text for details.

The thin X-ray windows were melted to quartz glass tubes that were used to seal the liquid sample volume against the laboratory environment by a set of Viton O-rings. The glass tube was sealed against the environment by a cascade of Viton O-rings that could be compressed with a fixing bolt from outside (see Fig. 2). Care was taken to ensure that the X-ray windows were exactly parallel in order to avoid thickness variations of the liquid in the X-ray beam which could alter or distort the measured spectra. Specially designed PTFE spacers of thickness 1–5 mm enabled a homogeneous distribution of the liquid between the windows, and an adjustment of the X-ray path length to the absorber concentration was also possible (see below). Besides the above-mentioned PTFE, the quartz glass windows and the Viton seals for the windows, no other materials were in direct contact with the $PbBr_2$ diethylene glycol solutions. The used quartz glass was extremely stable against the organic solvents, *i.e.* no changes of the solution were observable even for long-term experiments at about 473 K as observed by laboratory X-ray diffraction. In addition, extended tests have also shown that the Viton material is stable up to temperatures of about 473 K. Therefore any leakage from the seals and possible reactions with the air atmosphere are avoided and the solution under investigation is not contaminated. Owing to the goal that temperatures of about 473 K should be reached at the position of the samples, a silicon oil (polydimethylsiloxane, supplied by ABCR chemicals, Karlsruhe, Germany) was used for the thermostating of the cell. The cell was assembled from two basically identical half-cells (154 mm outer diameter, 45 mm length) which were hermetically closed and filled with the thermostating fluid in order to avoid any contamination of the solution. In addition, the hermetically closed Si-oil cycle was also essential for safety reasons. The liquid under investigation was kept in a small and variable volume (~2–4 cm^3) between the two half-cells as can be seen in detail in Fig. 2(*a*). Each half-cell consists of a large PTFE body with a plane surface on one side. On this side, the half cells and thus the liquid samples volume are sealed against each other by Viton O-rings. On the outer side, the half-cell is closed by a large brass cover, in which inlets and outlets for the thermostating Si oil are provided. For routine use, the half-cells are permanently connected to the thermostat in order to avoid a possible contamination of the inert inner parts of the cell with Si oil. In addition, the possible infiltration from air or humidity into the thermostating cycle is eliminated this way. The two half-cells are clamped together by 12 long threaded bars, and the liquid is introduced from the top of the cell *via* an injection channel. The cell design is optimized in order to achieve a good equilibration of the liquid with the thermostating fluid as shown in the sectional drawing in Fig. 2(*a*). The construction of the cell ensures that the liquid under investigation is completely surrounded by the large volume of the Si-oil heat reservoir. In addition, the X-ray windows are also thermalized by the Si oil

so that any possible precipitation of solid products from the solution on the windows is inhibited. A small Ni–CrNi thermocouple which was sealed in a glass tube was placed in the solution for its temperature measurement (see Fig. 2*b*). The stabilization of this temperature to an accuracy of about ± 0.1 K was achieved by a Pt1000 thermoresistor which was placed directly in the thermostating Si oil with a feedback loop to the thermostat. Compared with cell designs that have been published previously (*e.g.* Furenlid *et al.*, 1990; Villain *et al.*, 1993; Sanchez Marcos *et al.*, 1994), the ability to precisely control the temperature is a huge advantage, and the temperature distribution is extremely homogeneous.

In order to optimize the X-ray path for the transmission-mode X-ray absorption experiments, PTFE spacers with different lengths ranging from 1 to 5 mm were made to adjust the edge jump to the concentration of the dissolved species under investigation to a reasonable value. In addition, the construction of the cell guarantees that it can easily and quickly be disassembled (*i.e.* within a few minutes), and the container for the liquid can easily be cleaned in order to preserve reproducible and clean conditions for each individual experiment and sample preparation. Operation is even possible without any spacers; in this case the smallest achievable distance is about 0.2 mm. Furthermore, the X-ray path length through the solution can be adapted to the absorber element concentration even during the experiment. This is a major advantage compared with cells with a fixed path length (*e.g.* Furenlid *et al.*, 1990; Sanchez-Marcos *et al.*, 1994; Ragnarsdottir *et al.*, 1998), especially if several different absorption edges have to be measured for the same sample and under identical conditions (concentration, temperature *etc.*).

In Fig. 3, an example of a typical X-ray absorption spectrum obtained at 353 K is presented; the X-ray path length was 3 mm for this experiment and the corresponding Pb concentration was about 0.3 mol l^{-1}. As an additional outcome of the X-ray absorption experiments, the lead and the bromine concentrations can be calculated from the length of the X-ray path and the absorption jump at each of the investigated edges independently. The values derived in this way fit well to those which were determined by potentiometric titrations of the $PbBr_2$ solutions with EDTA (see Fig. 1; Oldag, 2000; Oldag *et al.*, 2005).

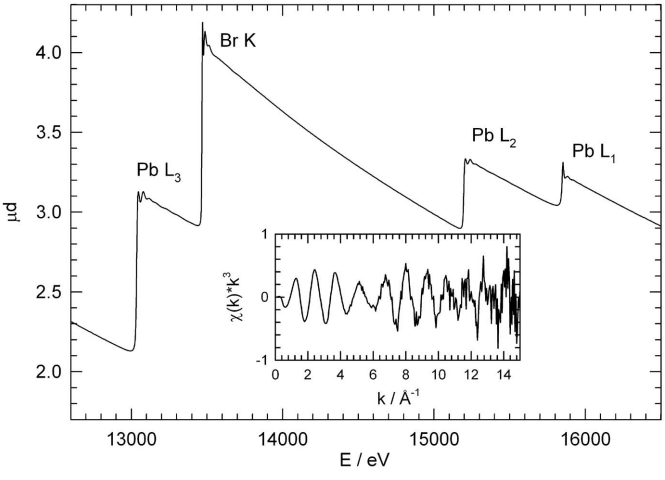

Figure 3
X-ray absorption spectrum covering the Pb *L*-edges and the Br *K*-edge of a solution of $PbBr_2$ in diethylene glycol for T = 353 K measured in the new *in situ* cell within about 90 min data acquisition time. In the inset, the extracted fine-structure oscillations $\chi(k)k^3$ at the Br *K*-edge are shown.

3. Experimental details

The X-ray absorption experiments presented here were performed at the bending-magnet station RÖMO II at the DORIS III storage ring at HASYLAB (DESY, Hamburg), operating at a positron energy of 4.43 GeV with injection currents of about 150 mA; more details about the design of this beamline including detection electronics *etc.* were given by Frahm (1989). The liquid samples were investigated in transmission mode in the *in situ* cell described above at the Pb *L*-edges (13035, 15200 and 15861 eV) and the Br *K*-edge (13474 eV) using N_2- and Ar-filled ionization chambers as detectors for the incoming and transmitted intensities. Typical scans cover the spectral range between 12600 and 16500 eV with about 2400 data points. A total acquisition time of $\sim$90 min was necessary for each single scan in order to achieve a reasonably high data quality. In order to use the available beam time as efficiently as possible we applied two identical experimental set-ups for two different experiments, one with the temperature increasing from 353 K to 433 K and the other with decreasing temperatures from 433 K to 353 K. While one sample was investigated with the X-ray beam, the second sample was thermally equilibrated in the second cell and *vice versa*. A Si(311) double-crystal monochromator was used, the crystals of which were detuned with respect to each other using a piezo crystal tilt stage to reduce the amount of harmonics in the Bragg-reflected beam (Materlik & Kostroun, 1980; Krolzig *et al.*, 1984). For the presented measurements, the monochromator was detuned to typically 60% of the maximum of the rocking curve. In the energy range used the photon flux through the slit system in front of the sample with an opening of about 10 mm (horizontally) and 0.5 mm (vertically) amounts to about 5×10^9 photons (see http://www-hasylab.desy.de/facility/experimental_stations/stations/X1.htm). A lead metal foil was measured between the second and a third ionization chamber in order to precisely calibrate the energy scale of the monochromator simultaneously with each sample. Data reduction and data analysis were performed according to standard procedures described in the literature (see, for example, Koningsberger & Prins, 1988) using the *Winxas* (Ressler, 1998), *AUTOBK* (Newville *et al.*, 1993), *FEFF* (Ankudinov *et al.*, 1998) and *FEFFIT* (Newville *et al.*, 1995) software packages.

A lead metal foil, crystalline $PbBr_2$ powder obtained from Fluka (Munich, Germany) and crystalline precipitates (*i.e.* $PbBr_2 \cdot C_4H_{10}O_3$ and $7\,PbBr_2 \cdot 8\,C_4H_{10}O_3$) pressed in polyethylene were measured in transmission to obtain reference spectra. For the preparation of the solutions, chemicals of p.a. quality were used. $PbBr_2$ (Fluka) of p.a. quality was crystal-

lized twice in 0.001 mol l^{-1} HBr and dissolved into vacuum-distilled diethylene glycol (Fluka) held at different temperatures. For the experiments described below, a solution of $PbBr_2$ in diethylene glycol saturated at 343 K was used in order to avoid any precipitation of solid products in the solution. The preparation of this solution involved an equilibration for 24–48 h in the presence of a significant amount of solid $PbBr_2$ while stirring the solution continuously. After sedimentation and decantation, the saturated liquid was transferred into the *in situ* cell within a couple of seconds without noticeable changes of the liquid's temperature.

4. Results and discussion

X-ray absorption measurements were performed for the upstream process (temperature variation from 353 to 433 K) and the downstream process (433 to 353 K). It has to be stressed here that this is the temperature region above the observed solubility maximum (see Fig. 1). For this purpose a solution saturated and equilibrated at 343 K was inserted into two different cells that were held at 353 and 433 K, respectively. In Fig. 3 an X-ray absorption measurement of a solution of $PbBr_2$ in diethylene glycol covering the spectral range of the Pb *L*-edges and the Br *K*-edge is presented for 353 K. The high data quality can be seen directly in the spectrum, as well as in the inset of this figure, where the extracted EXAFS fine-structure oscillations at the Br *K*-edge are presented. Although the Br concentration amounts to only $\sim$0.6 mol l^{-1}, fine-structure oscillations are clearly visible even above $k \simeq 15$ Å^{-1}. In Fig. 4(*a*) the temperature dependence of the Pb L_3 XANES spectra is depicted as an example; it should be mentioned that similar observations were made for the L_2- and the L_1-edges and the Br *K*-edge. While a slight decrease in the white-line intensity at 13047 eV can be observed, an increase in the absorption is visible for a photon energy of about 13060 eV. Similarly, the intensity of the absorption maximum at 13080 eV decreases and that of the minimum at 13100 eV increases as the temperature is increased from 353 to 433 K. In addition, small energy shifts of the absorption features are observed; for example, the white line shifts from 13047 eV at 353 K to 13048.5 eV at 433 K. The intensity of the white line at about 13047 eV photon energy is depicted as a function of the sample temperature in Fig. 4(*b*) for the upstream and the downstream processes.

One might argue that these small changes in the absorption coefficient as a function of temperature might be caused by anharmonic effects which are rather likely for molecules in solution (see, for example, Filipponi, 2001). However, such an anharmonic effect would be completely reversible with temperature and the observed differences in the absorption coefficients that were detected for the upstream and downstream processes (see Fig. 4*b*) cannot be explained by anharmonic effects only. Furthermore, a Fourier-transform analysis of the measured data clearly confutes that anharmonic effects are responsible for the observed effects as follows. In Fig. 5(*a*) we show the magnitude of the Fourier transforms (FTs) of the k^3-weighted fine-structure oscillations measured above the Br *K*-edge at 357 K for the upstream and the downstream process. Small but significant differences are observed between both spectra, indicating that a structural change has occurred in the solution in the heating/cooling cycle. In addition, a closer inspection of the XANES spectra in Fig. 4(*a*) reveals isobestic points at 13053, 13071 and 13088 eV, which suggests the presence of two different species in the organic solution that occur in varying concentrations as a function of the temperature.

For a more detailed analysis of the FTs presented in Fig. 5(*a*), it is first required to consider the reference compounds, especially crystalline $PbBr_2$ and $PbBr_2 \cdot C_4H_{10}O_3$, the FTs of which are presented in Fig. 5(*b*) in comparison with the spectrum of the solution measured at 357 K in the upstream direction. In the FT of $PbBr_2$, which crystallized in an orthorhombic structure (*Pnam*, No. 62; see Lumbreras *et al.*, 1986), the peak at $\sim$3 Å corresponds to the first Br–Pb coordination shell which extends over four subshells in 2.95–3.27 Å radial distance, and the smaller peak at 3.6 Å originates from a Br coordination sphere at about 3.65 Å. The broad peak at 2.3 Å is due to the resonating behaviour of the Pb backscattering amplitude and phase. Similar Br—Pb and Br—Br distances are observed for the Pb–Br precipitate $PbBr_2 \cdot C_4H_{10}O_3$ (monoclinic structure, $P12_1/n1$, No. 14). In contrast, all observed peaks in the FTs of the Pb–Br solutions (Fig. 5*a*) are located at smaller radii. From a detailed

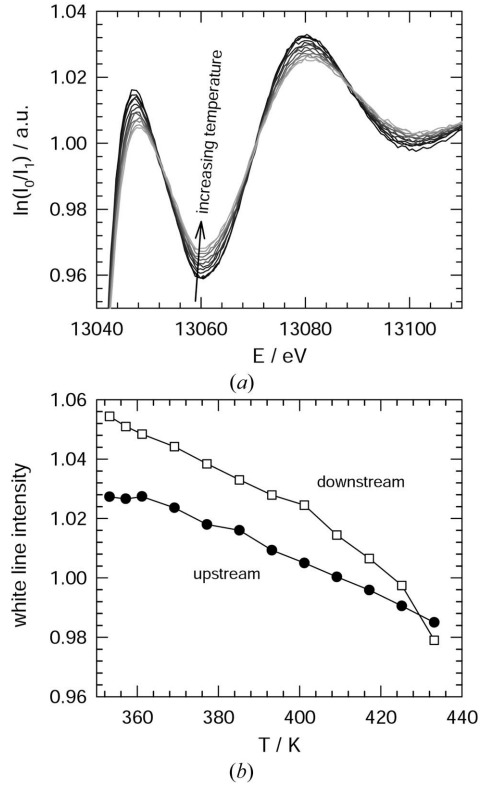

Figure 4
(*a*) Changes of the XANES structures at the Pb L_3-edge observed during the heating of the $PbBr_2$ diethylene glycol solutions from 353 to 433 K. (*b*) Variation of the white-line intensity at $\sim$13047 eV as a function of the temperature in the upstream (circles) and downstream (squares) processes.

comparison of the real and imaginary parts of FTs of the liquid solutions and the reference compounds, we concluded that both peaks in the FTs of the organic Pb–Br solution are due to Br–Pb interactions. Oxygen as well as carbon backscatterers are very unlikely: Br^- as well as O^{2-} are strongly electronegative and would therefore give rise to a strong repulsion force. Covalent Br—Br bonds are well known; however, such a dimeric bond is in strong contradiction to the Br *K*-edge position observed in the present study, *i.e.* $E_K = 13466$ eV. The latter is typical for a Br^- species and Br–Br dimers are expected to reveal a significant edge shift towards higher energies. Free carbon in an organic solution is not stable, and glycolic bonds are expected at much larger distances. In addition, fits with such low-*Z* backscattering elements never fit the imaginary part in the FTs sufficiently well.

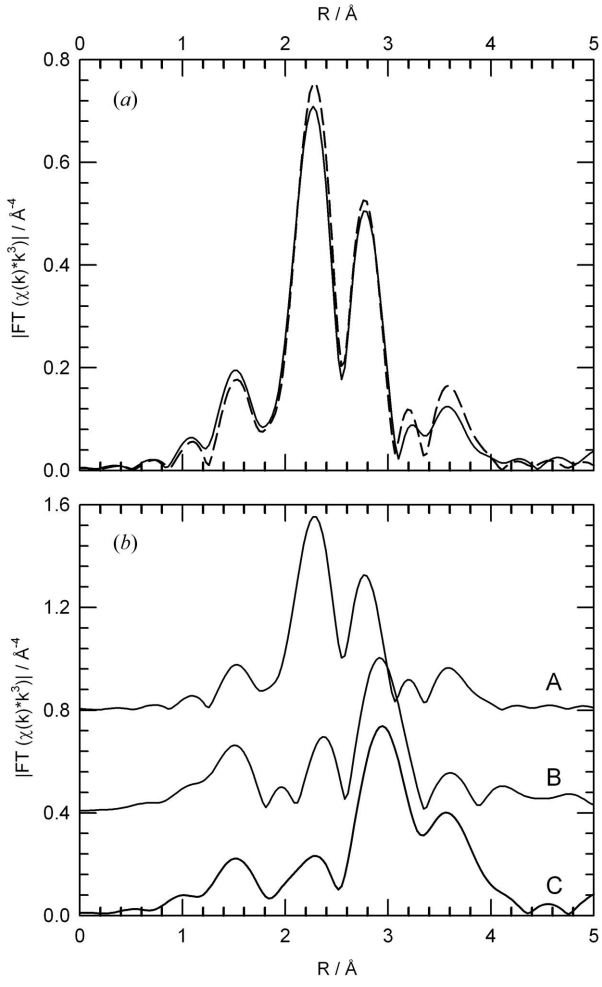

Figure 5
(*a*) FT magnitudes of the k^3-weighted extended X-ray absorption fine structures measured above the Br *K*-edge for a $PbBr_2$ solution in diethylene glycol at 357 K in the upstream (dashed line) and the downstream process after heating to 433 K and cooling to 357 K (solid line). (*b*) Comparison of k^3-weighted FT magnitudes of the extended X-ray absorption fine structures measured above the Br *K*-edge for several $PbBr_2$ reference compounds as indicated. A: solution at 357 K in the upstream process. B: solid crystalline $PbBr_2 \cdot C_4H_{10}O_3$. C: crystalline $PbBr_2$. Data are shifted vertically by 0.4 and are not corrected for phase shifts. FT in the range 2 Å^{-1}< k < 11.6 Å^{-1}.

We therefore modelled the experimental data using phases and amplitudes calculated for two species with different Br—Pb bond lengths by *FEFF*. The experimental data were fitted in *R* space between radial distances of 1.8 and 3.2 Å (2 Å^{-1} < k < 11 Å^{-1}). Typical fit results are presented in Fig. 6 for solutions at 357 and 425 K in the upstream direction. As can be seen, both the imaginary part of the FT as well as its magnitude are well reproduced in the region of the two shells by the calculations. In addition, it should be noted that the feature at a radial distance of ∼1.5 Å in the FT is well reproduced by the fit, which suggests that this spectral feature is also caused by the resonating behaviour of the phases and amplitudes of the backscattering atom. Since this region of the FT was not included in the fitting procedure, the observed agreement between data and fit in this radial distance can be interpreted as further proof of Pb backscattering atoms in the first Br coordination shells.

Fit results for four representative measurements at 357 K and 425 K are compiled in Table 1. As can be seen, the nearest

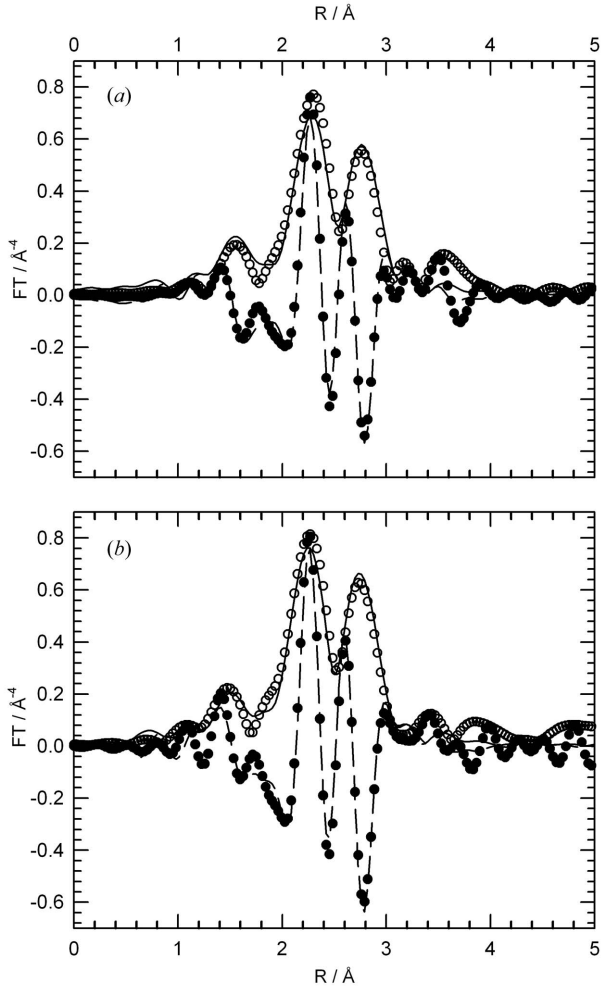

Figure 6
FT magnitude and imaginary part of the different k^3-weighted EXAFS spectra of $PbBr_2$ solutions in diethylene glycol at the Br *K*-edge for (*a*) T = 357 K and (*b*) T = 425 K. Dotted points indicate the experimental data, while the solid lines show the results of fitting with *FEFFIT*. (FT in the range 2 Å^{-1}< k < 11.6 Å^{-1}.)

Table 1
Structural parameters obtained by fitting the Br *K*-EXAFS spectra of the $PbBr_2$ diethylene glycol solutions using a model consisting of two individual Br–Pb species for two temperatures in the upstream and downstream process.

	First Br–Pb coordination			Second Br–Pb coordination		
	R_1 (Å)	N_1	σ_1^2 (10^{-3} Å^2)	R_2 (Å)	N_2	σ_2^2 (10^{-3} Å^2)
357 K upstream	2.45 ± 0.06	1.13 ± 1.31	23 ± 19	2.73 ± 0.03	1.15 ± 0.68	13 ± 6
425 K upstream	2.44 ± 0.06	0.85 ± 1.10	18 ± 16	2.71 ± 0.03	1.44 ± 0.67	14 ± 5
425 K downstream	2.44 ± 0.06	0.88 ± 1.14	20 ± 19	2.72 ± 0.02	1.33 ± 0.63	15 ± 5
357 K downstream	2.44 ± 0.03	0.98 ± 0.59	21 ± 9	2.73 ± 0.01	1.35 ± 0.37	15 ± 3

Pb neighbour distance appears at about 2.45 ± 0.05 Å and the second Pb shell is located at about 2.72 ± 0.03 Å. In particular, the first bond length is extremely short compared with, for example, Br—Pb distances in crystalline $PbBr_2$ or the precipitated $PbBr_2 \cdot C_4H_{10}O_3$ solid and will be the subject of further investigations in the future. While the fit results for the Debye–Waller factors (σ^2) do not vary significantly as a function of the temperature and the sample treatment, significant changes are observed for the coordination numbers of both shells. Starting at 357 K, the derived coordination numbers are almost identical for both shells, *i.e.* $N_1 \simeq N_2 \simeq 1.1$. It should be noted here that such a coordination number is rather likely for Br—Pb bonds in terms of the chemistry. At 425 K, however, a significantly increased value was found for the second shell ($N_2 \simeq 1.35$) and a decrease was found for N_1 (*i.e.* $N_1 \simeq 0.87$) for both the upstream and the downstream direction. These values were conserved when the solution was cooled to 357 K again, indicating that some of the bromine–lead coordinations have changed their local environment in the course of the heating/cooling cycle. It should be mentioned here that the errors given in Table 1, especially those corresponding to the coordination numbers, are partly as large as the respective quantities. Since we were only able to detect significant changes in the coordination numbers, we have fixed all other parameters in the fit procedure for test purposes, *i.e.* $R_1 = 2.45$ Å, $R_2 = 2.72$ Å, $\sigma_1^2 = \sigma_2^2 = 0.02$ Å^2. Fits that were performed with these restrictions, however, clearly affirm the results obtained before, but with significantly smaller confidence limits of about 5–10%. Therefore we think that the results presented in Table 1 are reasonable.

In conclusion, the obtained results suggest that part of the Br–Pb coordination of the solved complexes changes irreversibly over the course of a heating/cooling cycle in diethylene glycol between 353 and 433 K, *i.e.* the Br–Pb complex which is preferably formed at elevated temperatures remains, at least partly, stable also for lower temperatures. For the future, it is essential to understand this behaviour in detail. For this purpose, the EXAFS measured at the Pb absorption edges as well as those at the Br edge have to be fitted simultaneously in order to obtain a consistent picture of the solvated complexes as a function of the heat treatment. For example, the features observed in the Br *K*-edge FTs in a radial distance of about 3.3 Å are probably due to Br–Br interactions. On the basis of these results, XANES calculations using, for example, the *FEFF8* code (Ankudinov *et al.*, 1998) are highly desirable for larger clusters of solvated $PbBr^+$ ions in order to further confirm the proposed structures. Preliminary results using synthetic model complexes have shown that the white-line intensity and resulting XANES structures above the edge are extremely sensitive to the atomic details of the solvated complex under investigation (Keil *et al.*, 2005). In addition, experiments applying several heating/cooling cycles are promising in order to obtain a more detailed insight into the occurring reaction.

5. Conclusions and outlook

We present a new and very flexible *in situ* cell for investigations of liquid samples with X-rays at elevated temperatures. The cell is made of two identical half-cells, each of which is hermetically sealed with the thermostating Si oil. The temperature range from room temperature to ∼473 K is accessible for investigations. First *in situ* experiments with this cell were performed for investigation of the temperature-dependent structure and solubility of $PbBr_2$ in diethylene glycol. The obtained results show that temperature-dependent X-ray investigations are easily possible using the cell and that high-quality EXAFS data can be obtained in an acceptable time frame. Small changes of both the XANES and the EXAFS were measured at the Br *K*-edge and Pb L_3-, L_2- and L_1-edges as a function of the sample temperature.

Our measurements suggest that the local structure of the organic $PbBr_2$ solution changes as a function of the temperature. The observed changes cannot be explained by anharmonic effects only, and it was concluded that a partly irreversible chemical reaction takes place during heating of a saturated Pb–Br solution from 353 to 433 K. Measurements at the Br *K*-edge indicated that the population of the second Br–Pb coordination shell increases at the expense of the first, *i.e.* Pb seems to be increasingly positioned in a more relaxed position, and this state seems to be preserved if the solution is cooled down again.

For the future, a more detailed analysis of the experimental data is planned, including a full structure determination of the Pb–Br complexes in solution and their changes as a function of the temperature (Keil *et al.*, 2005). Furthermore, additional investigations of $PbBr_2$ solutions in other solvents such as glycol, triethylene glycol, glyme, diglyme and triglyme are planned for the future. In particular, experiments with triethylene glycol seem to be promising because triethylene glycol reveals a solubility maximum similar to diethylene glycol. However, the maximum solubility is extremely high with values of more than 300 mg ml^{-1}, *i.e.* more than twice those of $PbBr_2$ in diethylene glycol. In addition, the *in situ*

combination of EXAFS measurements with other spectroscopic techniques such as Raman spectroscopy seems to be very promising (Briois *et al.*, 2005).

This project was supported by the MWF Nordrhein-Westfalen. The provision of beam time and additional support by HASYLAB is gratefully acknowledged.

References

Ankudinov, A. L., Ravel, B., Rehr, J. J. & Conradson, S. D. (1998). *Phys. Rev. B*, **58**, 7565–7576.

Briois, V., Belin, S., Villain, F., Bouamrane, F., Lucas, H., Lescouëzec, R., Julve, M., Verdaguer, M., Tokumoto, M. S., Santilli, C. V., Pulcinelli, S. H., Carrier, X., Krafft, J. M., Jubin, C. & Che, M. (2005). *Phys. Scr.* In the press.

Charnock, J. M., Henderson, C. M. B. & Seward, T. M. (1999). *J. Synchrotron Rad.* **6**, 607–608.

Della Longa, S., Bianconi, A., Brancaccio, A., Brunori, M., Congiu Castellano, A., Cutruzzola, F., Hazemann, J. L., Missori, M. & Travaglini-Allocatelli, C. (1995). *Physica B*, **208/209**, 743–745.

Denecke, M. A., Reich, T., Pompe, S., Bubner, M., Heize, K. H., Nitsche, H., Allen, P. G., Bucher, J. J., Edelstein, N. M., Shuh, D. K. & Czerwinski, K. R. (1998). *Radiochim. Acta*, **82**, 103–109.

Farges, F., Sharps, J. A. & Brown, G. E. (1993). *Geochim. Cosmochim. Acta*, **57**, 1243–1252.

Filipponi, A. (2001). *J. Phys. Condens. Matter*, **13**, R23–R60.

Filipponi, A. & Di Cicco, A. (1994). *Nucl. Instrum. Methods B*, **93**, 302–310.

Filipponi, A., Ottaviano, L., Passacantando, M., Picozzi, P. & Santucci, S. (1993). *Phys. Rev. E*, **48**, 4575–4583.

Frahm, R. (1989). *Rev. Sci. Instrum.* **60**, 2515–2518.

Furenlid, L. R., Renner, M. W. & Fajer, J. (1990). *Rev. Sci. Instrum.* **61**, 1326–1327.

Gharia, A. C., Joshi, S. K., Shrivastava, B. D. & Khadikar, P. V. (1995). *Physica B*, **208/209**, 737–738.

Hertz, W. & Hellebrandt, M. (1923). *Z. Anorg. Allg. Chem.* **130**, 188–192.

Keil, P., Oldag, T., Lützenkirchen-Hecht, D., Keller, H.-L. & Frahm, R. (2005). In preparation.

Kemner, K. M., Elam, W. T., Hunter, D. B. & Bertsch, P. M. (1995). *Physica B*, **208/209**, 735–736.

Koningsberger, D. C. & Prins, R. (1988). Editors. *X-ray Absorption: Principles, Applications, Techniques of EXAFS, SEXAFS and XANES*. New York: John Wiley and Sons.

Kortright, J., Warburton, W. & Bienenstock, A. (1983). *EXAFS and Near-Edge Structures*, edited by A. Bianconi, L. Incoccia and S. Stipcich, pp. 362–372. Berlin, Heidelberg: Springer Verlag.

Krolzig, A., Materlik, G., Swars, M. & Zegenhagen, J. (1984). *Nucl. Instrum. Methods*, **219**, 430–434.

Licheri, G. & Pinna, G. (1983). *EXAFS and Near-Edge Structures*, edited by A. Bianconi, L. Incoccia and S. Stipcich, pp. 240–247. Berlin, Heidelberg: Springer Verlag.

Lumbreras, M., Protas, J., Jebbari, S., Dirksen, G. J. & Schoonman, J. (1986). *Solid State Ion.* **20**, 295–304.

Lützenkirchen-Hecht, D. & Frahm, R. (2001). *J. Phys. Chem. B*, **105**, 9988–9993.

Lützenkirchen-Hecht, D., Waligura, C. U. & Strehblow, H.-H. (1998). *Corros. Sci.* **40**, 1037–1042.

Materlik, G. & Kostroun, V. (1980). *Rev. Sci. Instrum.* **51**, 86–94.

Newville, M., Livins, P., Yacoby, Y., Stern, E. A. & Rehr, J. J. (1993). *Phys. Rev. B*, **47**, 14126–14131.

Newville, M., Ravel, B., Haskel, D., Rehr, J. J., Stern, E. A. & Yacoby, Y. (1995). *Physica B*, **208/209**, 154–155.

Oelkers, E. H., Sherman, D. M., Ragnarsdottir, K. V. & Collins, C. (1998). *Chem. Geol.* **151**, 21–27.

Oldag, T. (2000). Diploma thesis, Universität Dortmund, Germany. (In German.)

Oldag, T., Kockelmann, W. & Keller, H.-L. (2005). *Z. Anorg. Chem.* In the press.

Ottaviano, L., Filipponi, A. & Di Cicco, A. (1994). *Phys. Rev. B*, **49**, 11749–11758.

Palinkas, G. & Kalman, E. (1981). *Diffraction Studies on Non-Crystalline Substances*, edited by I. Hargittai and W. J. Orville-Thomas, pp. 293–373. Amsterdam: Elsevier Science.

Ragnarsdottir, K. V., Oelker, E. H., Sherman, D. M. & Collins, C. R. (1998). *Chem. Geol.* **151**, 29–39.

Ressler, T. (1998). *J. Synchrotron Rad.* **5**, 118–122. (See also www.winxas.de.)

Riggs-Gelasco, P. J., Stemmler, T. L. & Penner-Hahn, J. E. (1995). *Coord. Chem. Rev.* **144**, 245–286.

Rothe, J., Denecke, M. A., Neck, V., Müller, R. & Kim, J. I. (2002). *Inorg. Chem.* **41**, 249–258.

Sanchez Marcos, E., Gil, M., Martinez, J. M. & Munoz-Paez, A. (1994). *Rev. Sci. Instrum.* **65**, 2153–2154.

Schneider, M. S., Grunwaldt, J.-D., Bürgi, T. & Baiker, A. (2003). *Rev. Sci. Instrum.* **74**, 4121–4128.

Schultz, E., Bertagnolli, H. & Frahm, R. (1990). *J. Chem. Phys.* **92**, 667–672.

Seward, T. M., Henderson, C. M. B., Charnock, J. M. & Dobson, B. R. (1996). *Geochim. Cosmochim. Acta*, **60**, 2273–2282.

Tsutsui, Y., Sugimoto, K., Wasada, H., Inada, Y. & Funahashi, S. (1997). *J. Phys. Chem. A*, **101**, 2900–2905.

Villain, F., Briois, V., Castro, I., Helary, C. & Verdaguer, M. (1993). *Anal. Chem.* **65**, 2545–2548.

Yachandra, V. K., Sauer, K. & Klein, M. P. (1996). *Chem. Rev.* **96**, 2927–2950.